OFFICE OF NAVAL RESEARCH
CONTRACT NONR-220(58)
NR-064-431

TECHNICAL REPORT NO. 18

ELASTOSTATIC LOAD–TRANSFER TO A HALF–SPACE FROM A PARTIALLY EMBEDDED AXIALLY LOADED ROD

BY
ROKURO MUKI AND ELI STERNBERG

DIVISION OF ENGINEERING AND APPLIED SCIENCE
CALIFORNIA INSTITUTE OF TECHNOLOGY
PASADENA, CALIFORNIA

APRIL 1969

Office of Naval Research
Contract Nonr-220(58)
NR-064-431

Technical Report No. 18

Elastostatic load-transfer to a half-space from a partially embedded axially loaded rod

by

Rokuro Muki and Eli Sternberg

Division of Engineering and Applied Science
California Institute of Technology
Pasadena, California
April 1969

Elastostatic load-transfer to a half-space from a partially embedded axially loaded rod*

by

Rokuro Muki and Eli Sternberg
University of California at Los Angeles
and
California Institute of Technology

Abstract

This investigation is concerned with the diffusion of an axial load from a bar of arbitrary uniform cross-section that is immersed in, up to a finite depth, and bonded to a semi-infinite solid of distinct elastic properties. The bar is perpendicular to the plane boundary of the embedding medium. The determination of the desired resultant force in the submerged bar-segment is reduced to a Fredholm integral equation by means of an approximative scheme developed and tested earlier in connection with a more elementary three-dimensional load-transfer problem. Extensive numerical results illustrating the decay of the bar-force, appropriate to various choices of the governing geometric and material parameters, are presented for the particular case of a bar of circular cross-section.

Introduction

Two-dimensional load-transfer problems, such as those occasioned by the diffusion of load from an elastic stringer into a

*The results communicated in this paper were obtained in the course of an investigation conducted under Contract Nonr-220(58) with the Office of Naval Research in Washington, D. C.

coplanar elastic sheet, have attracted repeated attention, chiefly because of their relevance to the stress analysis and design of aircraft structures. The rather extensive literature on problems in this category goes back in its origins to a fundamental paper by Melan [1], in which he dealt with the transfer of an axial load from an infinite stringer to an all-around infinite elastic sheet[1]. The problem concerning the transmission of an axial load from a transverse stringer (tension-bar), a finite segment of which overlaps with, and is continuously bonded to, a semi-infinite elastic sheet, was initially posed by Reissner [2]. References to related publications are to be found in [3], [4], [5], which contain some recent contributions bearing on Melan's and Reissner's problems.

The diffusion of load from a bar into a three-dimensional elastic medium presents appreciably greater analytical difficulties. A comparatively simple, if somewhat artificial, example of this kind is supplied by the spatial analogue of Melan's problem, investigated in [6]. There we considered an infinite cylindrical bar fully immersed in, and continuously bonded to, an elastic medium of distinct mechanical properties occupying the remainder of the space; the bar was assumed to be subjected to an axial loading, confined to, and uniformly distributed over, one of its cross-sections. Our objective consisted in determining the decay of the resultant bar-force induced by the given loading. This task was performed rigorously, within three-dimensional elastostatics, for the special case of a bar of circular cross-section. The results thus obtained were then compared

---

1) Within Melan's approximate formulation, this problem is mathematically equivalent to the one in which the stringer is attached to the edge of an elastic sheet occupying a half-plane.

and found to be in favorable agreement, with those deduced in [6] by an approximate method that is applicable to a bar of arbitrary cross-section.

The work summarized in [6] was undertaken primarily as a pilot study for the present investigation of the three-dimensional counterpart of Reissner's problem, which may be described as follows. A finite or semi-infinite elastic bar of arbitrary uniform cross-section is immersed in, up to a finite depth, and continuously bonded to, an elastic half-space of different material properties, the cylindrical boundary of the bar being perpendicular to the plane boundary of the half-space. The applied loading is confined to the projecting portion of the bar and is taken to be statically equivalent to a centroidal axial force. We seek the decay of the resultant bar-force in the embedded portion of the bar, as a measure of the diffusion of the applied load into the surrounding semi-infinite medium. This problem is one of basic importance in structural engineering and soil mechanics because of its interest in connection with anchor bars and pile-supported buildings. Moreover, its solution is not readily accessible by rigorous means even for a bar of circular cross-section.

The approximative scheme employed by Melan, and later adopted by Reissner, in dealing with the plane load-transfer problems considered in [1] and [2], respectively, has no direct analogue in the analysis of the corresponding spatial problems. To make this clear we recall first the simplifying assumptions underlying [1], [2]. In both instances the bar is modeled as a one-dimensional elastic continuum, whereas the sheet is treated as a two-dimensional elastic

medium within the conventional theory of generalized plane stress. Consequently, both Melan and Reissner regard the bond-forces exerted by the stringer on the sheet as an ideal line-load and impose as a bond condition the requirement that the axial strain in the bar match the appropriate extensional strain in the sheet. This condition, with the aid of the familiar two-dimensional singular solutions pertaining to a concentrated load at an interior point of an infinite or semi-infinite elastic sheet, leads to a singular integro-differential equation for the desired bar-force, the integral thus emerging being convergent in the sense of its Cauchy principal value.

A strictly one-dimensional bar-model, in conjunction with a bond condition based on the assumption of ideal line-contact, is no longer feasible in dealing with the transfer of load into a three-dimensional elastic medium: here, in contrast to the situation encountered in two dimensions, the strain field due to a line-load is unbounded along the line-segment of load-application[1]. Indeed, the formal analogue of Melan's formulation in the present circumstances gives rise to a bond condition that involves a divergent integral and is therefore devoid of meaning.

To circumvent the difficulty described above, it is essential to amend Melan's assumptions. A suitable approximate formulation of the present problem is given in Section 1. This formulation is based on an adaptation of the approximative scheme devised in [6], which was in turn suggested by a corresponding treatment of Reissner's

---

1) Recall that the strain singularity associated with a concentrated load in three-space is one order higher than its two-dimensional counterpart.

plane problem, carried out in [5][1]. The remainder of the section is devoted to reducing the determination of the desired resultant force in the bar to the solution of an integral equation of Fredholm's second kind. An essential tool for the analysis in Section 1 is supplied by Mindlin's [7] solution to the problem of a concentrated load acting at an interior point of an elastic half-space[2].

In Section 2 we specialize the characterization of the bar-force deduced in Section 1 for the particular, physically most significant, case of a bar of circular cross-section. Here we also establish certain asymptotic properties of the solution appropriate to the circular bar and present illustrative quantitative results based on the numerical solution of the Fredholm integral equation that governs the diffusion of the applied load in the present instance.

1. Approximate formulation of problem. Reduction to a Fredholm integral equation.

We proceed now to an approximate mathematical formulation of the three-dimensional analogue of Reissner's problem described in the Introduction. To this end, let $\{O; x_1, x_2, x_3\}$ be a rectangular cartesian coordinate frame (Figure 1) with the origin O, spanning the three-dimensional Euclidean space E. Further, let $\underset{\sim}{x}=(x_1, x_2, x_3)$ denote the position vector of points in E and call $\underset{\sim}{e}$ the unit base-vector in the x_3-direction.

Consider a finite or semi-infinite cylindrical elastic bar, the longitudinal centroidal axis of which coincides with the x_3-axis. We

---

1) See Section 3 of [5].

2) See Mindlin [8] for a systematic derivation of the solution to his problem.

call Π the generic open cross-sectional region of the bar and assume Π to be a bounded plane region, whose boundary[1] $\partial\Pi$ is a simple closed curve, consisting of a finite number of arcs with continuous curvature. Suppose H to be the open half-space given by

$$H=\{\underset{\sim}{x}\,|\,\underset{\sim}{x}\in E,\ x_3>0\}, \tag{1.1}$$

designate by D the (cylindrical)subdomain of H defined by

$$D=\{\underset{\sim}{x}\,|\,(x_1,x_2)\in\Pi,\ 0<x_3<\ell\}, \tag{1.2}$$

and set

$$\Pi_z=\{\underset{\sim}{x}\,|\,(x_1,x_2)\in\Pi,\ x_3=z\}\quad(0\le x_3\le\ell), \tag{1.3}$$

where Π_z is the open cross-section of $\overline{D}$ located at $x_3=z$. In particular, Π_o and Π_ℓ stand for the interiors of the terminal cross-sections of $\overline{D}$, situated at $x_3=0$ and $x_3=\ell$, respectively (Figure 1). Next, consider an elastic body ("embedding medium") whose interior occupies the domain $H-\overline{D}$ and suppose one end-portion of the bar occupies $\overline{D}$ and is continuously bonded to the surrounding solid throughout the interface $\partial D-\Pi_o$. Accordingly, D represents the interior of the embedded segment of the bar and ℓ is the length of this submerged segment. Finally, assume the entire loading is confined to the projecting portion of the bar and is statically equivalent to a force $-\underset{\sim}{e}p_o$ acting along the x_3-axis, so that $p_o>0$ corresponds to a tensile loading. We seek the resultant axial bar-force $p(x_3)$ $(0\le x_3\le\ell)$, which governs the load-diffusion into the embedding medium, on the assumption that the latter, as well as the bar itself, are homogeneous and isotropic linearly elastic solids of possibly distinct material properties. Let η and ν, in this order, stand for

---

[1] If S is a point-set in a Euclidean space of two or three-dimensions, we write $\overline{S}$ and ∂S for the closure and the boundary of S, respectively.

Young's modulus and Poisson's ratio of the embedding medium; Young's modulus of the bar[1] will be designated by η'.

The present approximate treatment of the problem aims at, and is confined in its physical relevance to, a bar with a maximum cross-sectional diameter that is suitably small compared to the length of the submerged bar-segment. As a first step we extend the embedding medium throughout the half-space $\overline{H}$ and consider an elastic body B in $\overline{H}$ with the elastic constants η, ν of the original material in $\overline{H}$-D. Next, we introduce a fictitious reinforcement B_* of the body B throughout the region D (Figure 2). The reinforcement B_* is chosen in such a way that the "composite solid" occupying D is "equivalent" to the actual immersed bar-segment B' in the sense that its extensional stiffness is the same as that of B'. We thus assign to the reinforcement B_* the modulus of elasticity η_* given by

$$\eta_*=\eta'-\eta\geq 0. \qquad (1.4)^2$$

In what follows we treat the extended embedding medium B as a three-dimensional elastic continuum within the framework of classical elastostatics. In contrast, we regard the fictitious reinforcement B_* as a one-dimensional elastic continuum as far as its constitutive law and equilibrium conditions are concerned. Accordingly, B_* is governed by the stress-strain relation

$$\frac{1}{A}p_*(z)=\eta_*\epsilon_*(z) \quad (0\leq z\leq \ell), \qquad (1.5)$$

if A is the area of Π, $p_*(z)$ is the scalar axial force in B_* at $x_3=z$, positive if tensile, and $\epsilon_*(z)$ is the associated axial strain. Further,

---

1) Poisson's ratio of the bar does not enter into the subsequent analysis.

2) Note that (1.4) rules out the practically uninteresting case in which $\eta'<\eta$.

the equilibrium requirement for B_* furnishes the differential equation

$$\dot{p}_*(z)+q(z)=0 \quad (0<z<\ell), \tag{1.6}$$[1]

where $\underset{\sim}{e}q(z)$ is the "bond-force" per unit bar-length exerted by B on B_* at $x_3=z$. In addition to the distributed bond-force of scalar density $q(z)$ $(0<z<\ell)$, B_* is subjected to the external axial forces $-\underset{\sim}{e}p_*(0)$ and $\underset{\sim}{e}p_*(\ell)$, concentrated within the terminal cross-sections $\overline{\Pi}_o$ and $\overline{\Pi}_\ell$, respectively: $-\underset{\sim}{e}p_*(0)$ is the portion of the applied load $-\underset{\sim}{e}p_o$ transmitted to B_* directly, whereas $\underset{\sim}{e}p_*(\ell)$ is the bond-force communicated by B to B_* at $x_3=\ell$ (See Figure 2).

The forces external with respect to the body B (extended matrix) consist of the distributed bond-forces of lineal density $-\underset{\sim}{e}q(z)$ $(0<z<\ell)$ exerted by B_* on B, together with the load-portion $-\underset{\sim}{e}[p_o-p_*(0)]$ transmitted to B directly at $x_3=0$ and the bond-force $-\underset{\sim}{e}p_*(\ell)$ concentrated within $\overline{\Pi}_\ell$. We assume the foregoing forces to be uniformly distributed over the respective cross-sections $\overline{\Pi}_z(0<z<\ell)$, $\overline{\Pi}_o$, and $\overline{\Pi}_\ell$ (See Figure 2).

Let σ_{ij} and ϵ_{ij} $(i,j=1,2,3)$ be the cartesian components of the fields of stress and strain induced in the body B by the system of external forces acting on B. Further, for every $\underset{\sim}{x}\in\overline{H}-\overline{\Pi}_\zeta$ and every $\zeta\in[0,\ell]$, let $\hat{\sigma}_{ij}(\underset{\sim}{x},\zeta)$ and $\hat{\epsilon}_{ij}(\underset{\sim}{x},\zeta)$ represent the stresses and strains at the point $\underset{\sim}{x}$ of the semi-infinite medium B due to a uniform body-force distribution over the closed disk $\overline{\Pi}_\zeta$, acting in the negative x_3-direction, the resultant applied force having unit magnitude. With the aid of these influence fields one has, for every point $\underset{\sim}{x}\in\overline{H}-\overline{\Pi}_o-\overline{\Pi}_\ell$,

$$\left.\sigma_{ij}(\underset{\sim}{x})=[p_o-p_*(0)]\hat{\sigma}_{ij}(\underset{\sim}{x},0)+p_*(\ell)\hat{\sigma}_{ij}(\underset{\sim}{x},\ell)+\int_0^\ell q(\zeta)\hat{\sigma}_{ij}(\underset{\sim}{x},\zeta)d\zeta,\right\} \tag{1.7}$$

---

[1] If v is a differentiable function of one variable, we write $\dot{v}$ for the derivative of v.

$$\left.\epsilon_{ij}(\underset{\sim}{x})=[p_o-p_*(0)]\hat{\epsilon}_{ij}(\underset{\sim}{x},0)+p_*(\ell)\hat{\epsilon}_{ij}(\underset{\sim}{x},\ell)+\int_0^{\ell}q(\zeta)\hat{\epsilon}_{ij}(\underset{\sim}{x},\zeta)d\zeta.\right\} \quad (1.7)\ \text{cont.}$$

Integral representations for the influence fields $\hat{\sigma}_{ij}$ and $\hat{\epsilon}_{ij}$ entering (1.7) are, in turn, immediately obtainable from Mindlin's [7], [8] solution for a concentrated load applied at a point of an elastic half-space. Indeed, designating by $\mathring{\sigma}_{ij}(\underset{\sim}{x},\zeta)$ and $\mathring{\epsilon}_{ij}(\underset{\sim}{x},\zeta)$ the stresses and strains of Mindlin's solution appropriate to the semi-infinite solid B and corresponding to the unit concentrated load in the negative x_3-direction applied at $(0,0,\zeta)$, one has

$$\hat{\sigma}_{ij}(\underset{\sim}{x},\zeta)=\frac{1}{A}\int_{\Pi_o}\mathring{\sigma}_{ij}(\underset{\sim}{x}-\underset{\sim}{\xi},\zeta)dA_{\underset{\sim}{\xi}}, \quad \hat{\epsilon}_{ij}(\underset{\sim}{x},\zeta)=\frac{1}{A}\int_{\Pi_o}\mathring{\epsilon}_{ij}(\underset{\sim}{x}-\underset{\sim}{\xi},\zeta)dA_{\underset{\sim}{\xi}}, \quad (1.8)^{1}$$

for all $\underset{\sim}{x}\in\overline{H}-\overline{\Pi}_{\zeta}$ $(0\le\zeta\le\ell)$. Explicit representations for $\mathring{\sigma}_{ij}$ and $\mathring{\epsilon}_{ij}$, in closed elementary form, will be cited later on.

Let p(z) be the desired axial bar-force at $x_3=z$ in the immersed bar segment B′. Then, within the approximation under consideration, p obeys

$$p(z)=p_*(z)+\int_{\Pi_z}\sigma_{33}(\underset{\sim}{x})dA \quad (0\le z\le\ell), \quad (1.9)$$

where $p(0)=p(0+)$ and $p(\ell)=p(\ell-)$. In order to render p fully determinate, one needs to adjoin to (1.9) a suitable bond condition that links the deformations of the fictitious reinforcing bar B_* and those of the extended embedding medium B. For this purpose we adopt the requirement that the axial strain $\epsilon_*(z)$ in B_* be equal to the cross-sectional average over Π_z of the extensional strain $\epsilon_{33}(\underset{\sim}{x})$ in B. Consequently,

---

1) Here and in the sequel the subscript attached to the element of area indicates the variable of integration.

$$\epsilon_*(z)=\frac{1}{A}\int_{\Pi_z}\epsilon_{33}(\underset{\sim}{x})dA \quad (0\le z\le \ell), \tag{1.10}$$

with the understanding that the integral in (1. 10) for z=0 and z=ℓ is to be interpreted in the sense of its corresponding limits as z→0 and z→ℓ from the interior of the interval $[0, \ell]$. Equations (1. 5) to (1. 10) suffice to characterize p(z) completely over the range $0\le z\le \ell$.

With a view toward making the foregoing characterization of the bar-force p more explicit, we define the auxiliary influence functions σ and ϵ through

$$\left.\begin{aligned}\sigma(z,\zeta)&=\frac{1}{A}\int_{\Pi_z}\hat{\sigma}_{33}(\underset{\sim}{x},\zeta)dA \quad (0\le z\le \ell,\ 0\le\zeta\le\ell,\ z\ne\zeta),\\ \epsilon(z,\zeta)&=\frac{1}{A}\int_{\Pi_z}\hat{\epsilon}_{33}(\underset{\sim}{x},\zeta)dA \quad (0\le z\le \ell,\ 0\le\zeta\le\ell,\ z\ne\zeta),\end{aligned}\right\} \tag{1.11}$$

supplemented by

$$\left.\begin{aligned}\sigma(0,0)&=\sigma(0+,0),\quad \sigma(\ell,\ell)=\sigma(\ell-,\ell),\\ \epsilon(0,0)&=\epsilon(0+,0),\quad \epsilon(\ell,\ell)=\epsilon(\ell-,\ell).\end{aligned}\right\} \tag{1.12}$$

It will be shown subsequently that the limits involved in (1. 12) exist. Further, $\sigma(z,\zeta)$ and $\epsilon(z,\zeta)$, regarded as functions of ζ, will be found to possess merely finite jump discontinuities at ζ=z for each fixed z in the open interval $(0, \ell)$. The physical significance of σ and ϵ as stress and strain averages associated with the influence fields $\hat{\sigma}_{ij}$ and $\hat{\epsilon}_{ij}$ is immediate from (1. 11), (1. 12).

We now substitute for $\sigma_{33}(\underset{\sim}{x})$, $\epsilon_{33}(\underset{\sim}{x})$ from (1. 7) into (1. 9), (1. 10) and – after a permissible reversal in the order of the two integrations – invoke (1. 11), (1. 12), as well as (1. 5), (1. 6), to arrive at

$$p(z)=p_*(z)+A\Big\{[p_o-p_*(0)]\sigma(z,0)$$

$$+p_*(\ell)\sigma(z,\ell)-\int_0^{\ell}\dot{p}_*(\zeta)\sigma(z,\zeta)d\zeta\Big\}\quad(0\le z\le\ell),\qquad(1.13)$$

$$\frac{1}{A\eta_*}p_*(z)=[p_o-p_*(0)]\epsilon(z,0)$$

$$+p_*(\ell)\epsilon(z,\ell)-\int_0^{\ell}\dot{p}_*(\zeta)\epsilon(z,\zeta)d\zeta\quad(0\le z\le\ell).\qquad(1.14)^{1}$$

Observe that the influence functions σ and ϵ are computable, for a bar of given cross-section Π, from (1.11), (1.12) in conjunction with (1.8) and Mindlin's solution [7]. Hence (1.14) constitutes an integro-differential equation for the fictitious bar-force p_*. Moreover, once $p_*(z)$ $(0\le z\le\ell)$ is known, the actual bar-force $p(z)$ $(0\le z\le\ell)$ follows from (1.13).

Our next objective is to reduce (1.14) to an ordinary integral equation of Fredholm's second kind and, at the same time, to transform (1.13) into a more convenient form. In order to accomplish this purpose we require more detailed information as to the structure of the influence functions σ and ϵ, which are related through (1.8), (1.11) to Mindlin's [7] solution. The latter furnishes for every $\zeta\in[0,\ell]$ and every $\underset{\sim}{x}\in\overline{H}$ $(\underset{\sim}{x}\neq\underset{\sim}{e}\zeta)$,

$$\overset{*}{\sigma}_{33}(\underset{\sim}{x},\zeta)=\frac{1}{8\pi(1-\nu)}\Big\{2(1-\nu)v_1(\underset{\sim}{x}-\underset{\sim}{e}\zeta)-(x_3-\zeta)v_2(\underset{\sim}{x}-\underset{\sim}{e}\zeta)$$

$$+2(1-\nu)v_1(\underset{\sim}{x}+\underset{\sim}{e}\zeta)-[(3-4\nu)x_3+\zeta]v_2(\underset{\sim}{x}+\underset{\sim}{e}\zeta)+2\zeta x_3v_3(\underset{\sim}{x}+\underset{\sim}{e}\zeta)\Big\},\quad(1.15)$$

---

1) In deducing (1.14) we excluded the degenerate case $\eta_*=0$, i.e., $\eta'=\eta$, which requires separate attention. We shall return to this case at the end of Section 1.

$$\dot{\epsilon}_{33}(\underset{\sim}{x},\zeta)=\frac{1+\nu}{8\pi(1-\nu)\eta}\Big\{2(1-2\nu)v_1(\underset{\sim}{x}-\underset{\sim}{e}\zeta)-(x_3-\zeta)v_2(\underset{\sim}{x}-\underset{\sim}{e}\zeta)$$

$$+2(1-2\nu)^2 v_1(\underset{\sim}{x}+\underset{\sim}{e}\zeta)-[(3-4\nu)x_3+(1-4\nu)\zeta]v_2(\underset{\sim}{x}+\underset{\sim}{e}\zeta)+2\zeta x_3 v_3(\underset{\sim}{x}+\underset{\sim}{e}\zeta)\Big\}, \quad (1.16)$$

where

$$v_n(\underset{\sim}{x})=-\frac{\partial^n}{\partial x_3^n}\left(\frac{1}{|\underset{\sim}{x}|}\right) \quad (n=1,2,3). \quad (1.17)$$

We now define functions U and V_n (n=1, 2, 3) by means of

$$\left.\begin{aligned} U(\underset{\sim}{x})&=-\frac{1}{A}\int_{\Pi_o}\frac{dA_{\underset{\sim}{\xi}}}{|\underset{\sim}{x}-\underset{\sim}{\xi}|} \text{ for all } \underset{\sim}{x}\in E,\\ V_n(\underset{\sim}{x})&=\frac{\partial^n}{\partial x_3^n}U(\underset{\sim}{x}) \text{ for all } \underset{\sim}{x}\in E-\overline{\Pi}_o \ (n=1,2,3). \end{aligned}\right\} \quad (1.18)$$

Thus U is the Newtonian potential of a uniform mass distribution of density -1/A over the disk $\overline{\Pi}_o$. From (1. 18) follows, for every $\underset{\sim}{x}\in E-\overline{\Pi}_o$,

$$\left.\begin{aligned} V_1(\underset{\sim}{x})&=\frac{x_3}{A}\int_{\Pi_o}\frac{dA_{\underset{\sim}{\xi}}}{|\underset{\sim}{x}-\underset{\sim}{\xi}|^3}, \quad V_2(\underset{\sim}{x})=\frac{1}{A}\int_{\Pi_o}\frac{|\underset{\sim}{x}-\underset{\sim}{\xi}|^2-3x_3^2}{|\underset{\sim}{x}-\underset{\sim}{\xi}|^5}dA_{\underset{\sim}{\xi}},\\ V_3(\underset{\sim}{x})&=\frac{3x_3}{A}\int_{\Pi_o}\frac{5x_3^2-3|\underset{\sim}{x}-\underset{\sim}{\xi}|^2}{|\underset{\sim}{x}-\underset{\sim}{\xi}|^7}dA_{\underset{\sim}{\xi}}. \end{aligned}\right\} \quad (1.19)$$

Finally, we introduce functions W_n (n=1, 2, 3) by setting

$$W_n(z)=\frac{1}{A}\int_{\Pi_z}V_n(\underset{\sim}{x})dA \quad (0<|z|<\infty), \quad (n=1,2,3). \quad (1.20)$$

As is readily confirmed with the aid of (1. 8), (1. 11) and (1. 15), (1. 16), (1. 17), by recourse to (1. 18), (1. 20), the functions σ and ϵ admit the representations

$$\sigma(z,\zeta)=\frac{1}{8\pi(1-\nu)}\{2(1-\nu)W_1(z-\zeta)-(z-\zeta)W_2(z-\zeta)+2(1-\nu)W_1(z+\zeta)$$

$$-[(3-4\nu)z+\zeta]W_2(z+\zeta)+2\zeta zW_3(z+\zeta)\}\quad(0\le z\le l,\ 0\le\zeta\le l,\ z\neq\zeta),\qquad(1.21)$$

$$\epsilon(z,\zeta)=\frac{1+\nu}{8\pi(1-\nu)\eta}\{2(1-2\nu)W_1(z-\zeta)-(z-\zeta)W_2(z-\zeta)+2(1-2\nu)^2W_1(z+\zeta)$$

$$-[(3-4\nu)z+(1-4\nu)\zeta]W_2(z+\zeta)+2\zeta zW_3(z+\zeta)\}\quad(0\le z\le l,\ 0\le\zeta\le l,\ z\neq\zeta).\qquad(1.22)$$

The behavior of the functions σ and ϵ is accordingly governed by, and may be inferred from, the properties of W_n (n=1, 2, 3) given by (1.19), (1.20). The functions W_n, in turn, are evidently continuous and possess continuous partial derivatives of all orders at all points of the real axis with the exception of the origin. Moreover, (1.19), (1.20) permit one to show that

$$W_1(0+)=-W_1(0-)=\frac{2\pi}{A},\quad\lim_{z\to0}\left[z^{n-1}W_n(z)\right]=0\ (n=2,3).\qquad(1.23)^{1}$$

Now let f and g be functions defined by

$$\left.\begin{aligned}\sigma(z,\zeta)&=\frac{1}{2A}[h(z-\zeta)+f(z,\zeta)]\quad(0\le z\le l,\ 0\le\zeta\le l,\ z\neq\zeta),\\ \epsilon(z,\zeta)&=\frac{1+\nu}{2(1-\nu)\eta A}[(1-2\nu)h(z-\zeta)+g(z,\zeta)]\quad(0\le z\le l,\ 0\le\zeta\le l,\ z\neq\zeta),\end{aligned}\right\}\qquad(1.24)$$

where

$$h(z)=1\ (0<z<\infty),\quad h(z)=-1\ (-\infty<z<0).\qquad(1.25)$$

It is clear from (1.21), (1.22), (1.23) and the regularity properties of W_n (n=1, 2, 3) described above that f and g so defined are continuously differentiable on the slit square

$$S=\{(z,\zeta)\,|\,0\le z\le l,\ 0\le\zeta\le l,\ z\neq\zeta\}\qquad(1.26)$$

---

1) See the Appendix at the end of the paper for a sketch of a proof of (1.23).

and coincide on S with functions continuous on the closed square $\bar{S}$. Consequently, the partial derivatives $\partial f/\partial\zeta$ and $\partial g/\partial\zeta$, for each fixed $z\in[0,\ell]$, are integrable functions of ζ on $[0,\ell]$.

At this stage we substitute for σ and ε from (1.24) into (1.13), (1.14), bearing in mind (1.12). We then apply an integration by parts to the integrals appearing (1.13), (1.14), taking proper account of the jump discontinuities[1] inherent in the step-function h. This procedure, which derives its legitimacy from the previously established regularity properties of f and g – provided the unknown function p_* (fictitions bar-force) is assumed to be continuously differentiable on $(0,\ell)$ and continuous on the closed interval $[0,\ell]$ – yields after an elementary computation.

$$\left[\frac{1}{\eta_*}+\frac{(1+\nu)(1-2\nu)}{(1-\nu)\eta}\right]p_*(z)-\frac{1+\nu}{2(1-\nu)\eta}\int_0^{\ell}p_*(\zeta)\frac{\partial}{\partial\zeta}g(z,\zeta)d\zeta$$

$$=\frac{(1+\nu)p_o}{2(1-\nu)\eta}[1-2\nu+g(z,0)]\quad(0\le z\le\ell),\qquad(1.27)$$

$$p(z)=\frac{p_o}{2}[1+f(z,0)]+\frac{1}{2}\int_0^{\ell}p_*(\zeta)\frac{\partial}{\partial\zeta}f(z,\zeta)d\zeta\quad(0\le z\le\ell).\qquad(1.28)$$

For a specified cross-section Π of the original bar, explicit integral representations of the functions f and g entering (1.27), (1.28) are obtainable from their definitions in (1.24) together with (1.19) to (1.22). Equation (1.27) is therefore an integral equation of Fredholm's second kind for the fictitious bar-force p_*. This integral equation is readily amenable to a numerical solution. Once p_* has been found, the

---

1) See the definition (1.25) of h. The range of integration $[0,\ell]$ needs to be decomposed into the subintervals $[0,z]$ and $[z,\ell]$.

actual bar-force p – which is the primary unknown in the problem under consideration – is determined by (1.28).

The value of p(0) may be extracted directly from (1.28). For this purpose observe from (1.11), (1.8) that

$$\sigma(0, \zeta)=0 \ (0<\zeta\leq l). \tag{1.29}$$

Now (1.29), (1.24), in view of the regularity properties of f established earlier, lead to

$$\frac{\partial}{\partial \zeta} f(z, \zeta)\Big|_{z=0}=\frac{d}{d\zeta} f(0, \zeta)=0 \ (0<\zeta\leq l), \quad f(0+, 0)=1. \tag{1.30}$$

Consequently, (1.28) implies

$$p(0)=p_o, \tag{1.31}$$

so that – in contrast to the situation encountered in the analogous treatment of Reissner's plane problem[1] – no concentrated load-transfer occurs at z=0.

Equation (1.27) is inapplicable[2] for $\eta_*=\eta'-\eta=0$, i.e., when the bar and the surrounding solid have the same modulus of elasticity. In this degenerate instance $p_*=0$ on $[0, l]$ according to (1.5), and thus (1.28), because of the last of (1.30), gives way to

$$p(z)=\frac{p_o}{2}[1+f(z, 0)] \ (0<z\leq l), \quad p(0)=p_o. \tag{1.32}$$

Finally, we note that elimination of q from the first of (1.7) with the aid of (1.6), and a subsequent integration by parts, lead to the representation

$$\sigma_{ij}(\underset{\sim}{x})=p_o \delta_{ij}(\underset{\sim}{x}, 0)+\int_0^l p_*(\zeta) \frac{\partial}{\partial \zeta} \delta_{ij}(\underset{\sim}{x}, \zeta) d\zeta \ \text{ for all } \underset{\sim}{x}\in \overline{H}-\overline{D} \tag{1.33}$$

---

1) See Section 3 of [5].

2) See the footnote attached to (1.14).

of the stress field in the original embedding medium, the influence field δ_{ij} being known from (1.8) and Mindlin's solution [7].

2. Specialization to a bar of circular cross-section. Asymptotic and numerical results. Discussion.

In this section we specialize the characterization (1.27), (1.28) of the bar-force p by considering the particular case of a bar of circular cross-section. Thus, henceforth

$$\Pi=\{(x_1,x_2)\,|\,x_1^2+x_2^2<a^2\},\quad A=\pi a^2, \tag{2.1}$$

where "a" is the radius of the cross-section. With a view toward expressing the functions f and g entering (1.27), (1.28) in convenient explicit form, we set

$$\left.\begin{aligned} &x_1=r\cos\theta,\quad x_2=r\sin\theta\quad (0<r<\infty,\ 0\le\theta<2\pi),\\ &\xi_1=\rho\cos\varphi,\quad \xi_2=\rho\sin\varphi\quad (0<\rho<\infty,\ 0\le\varphi<2\pi), \end{aligned}\right\} \tag{2.2}$$

and recall that the Newtonian potential at (x_1,x_2,x_3) of a particle situated at $(\xi_1,\xi_2,0)$ admits the Laplace-integral[1] representation

$$[(x_1-\xi_1)^2+(x_2-\xi_2)^2+x_3^2]^{-1/2}=\int_0^\infty \exp(-|x_3|s)J_0(s\sqrt{r^2+\rho^2-2r\rho\cos(\theta-\varphi)})\,ds \tag{2.3}$$

for all $\underset{\sim}{x}\in E$ except $\underset{\sim}{x}=(\xi_1,\xi_2,0)$. Here J_0 is the zero-order Bessel function of the first kind. Consequently, the disk-potential U defined by the first of (1.18) may in the present instance be written as

$$U(\underset{\sim}{x})=-\frac{1}{\pi a^2}\int_0^a\int_0^{2\pi}\int_0^\infty \exp(-|x_3|s)J_0(s\sqrt{r^2+\rho^2-2r\rho\cos(\theta-\varphi)})\,\rho\,ds\,d\varphi\,d\rho \tag{2.4}$$

---

[1] Watson [9], p. 384.

for every $\underset{\sim}{x} \in E$. Next, recall the series expansion[1]

$$J_o(s\sqrt{r^2+\rho^2-2r\rho\cos(\theta-\varphi)}) = J_o(sr)J_o(s\rho) + 2\sum_{n=1}^{\infty} J_n(sr)J_n(s\rho)\cos[n(\theta-\varphi)], \qquad (2.5)$$

in which J_n denotes the Bessel function of the first kind of order n. Substituting from (2.5) into (2.4) and bearing in mind that

$$\int_0^a J_o(s\rho)\rho d\rho = \frac{a}{s} J_1(sa) \quad (0<s<\infty), \qquad (2.6)^2$$

one obtains, after a permissible interchange of the order of the integrations in (2.4) and upon a legitimate termwise integration with respect to φ,

$$U(\underset{\sim}{x}) = -\frac{2}{a}\int_0^{\infty} \frac{1}{s}\exp(-|x_3|s)J_o(sr)J_1(sa)ds \quad \text{for all } \underset{\sim}{x} \in E. \qquad (2.7)^3$$

Equation (2.7) in conjunction with the second of (1.18) now yields

$$V_n(\underset{\sim}{x}) = -\frac{2}{a}[-h(x_3)]^n \int_0^{\infty} s^{n-1}\exp(-|x_3|s)J_o(sr)J_1(sa)ds \quad \text{for all } \underset{\sim}{x} \in E-\partial H \ (n=1,2,3), \qquad (2.8)$$

where h is the step-function introducing in (1.25). Inserting V_n from (2.8) into (1.20) and carrying out the area-integration (over the circular region Π_z) under the improper integral, as is justified, one is led to

---

1) Watson [9], p. 358.

2) Watson [9], p. 18.

3) This integral representation for the Newtonian potential of a uniform circular disk is originally due to Weber [10].

$$W_n(z) = -\frac{4}{a^{n+1}}[-h(z)]^n R_n(|z|) \quad (0<|z|<\infty), \quad (n=1,2,3), \tag{2.9}$$

provided R_n, for every positive integer n, is the function defined by

$$R_n(t) = a^{n-1}\int_0^\infty s^{n-2}\exp(-ts)[J_1(as)]^2 ds \quad (0<t<\infty). \tag{2.10}$$

Evidently, R_n is continuous and has continuous partial derivatives of all orders on $(0,\infty)$.

It is clear from (2.9), (1.21), (1.22), that the influence functions σ and ϵ may now be expressed in terms of the integrals R_n (n=1,2,3), the step-function h, and elementary functions. Once this has been accomplished, the respective "continuous parts" f and g of σ and ϵ are obtainable directly from (1.24). In this manner one arrives at the following results for a bar of circular cross-section:

$$\left.\begin{aligned} f(z,\zeta) &= \frac{1}{1-\nu}\{(1-\nu)h(z-\zeta)[2R_1(|z-\zeta|)-1]+2(1-\nu)R_1(z+\zeta) \\ &\quad + \frac{z-\zeta}{a}R_2(|z-\zeta|)+[\frac{\zeta}{a}+(3-4\nu)\frac{z}{a}]R_2(z+\zeta)+\frac{2z\zeta}{a^2}R_3(z+\zeta)\}, \\ g(z,\zeta) &= (1-2\nu)h(z-\zeta)[2R_1(|z-\zeta|)-1]+2(1-2\nu)^2R_1(z+\zeta) \\ &\quad + \frac{z-\zeta}{a}R_2(|z-\zeta|)+[(1-4\nu)\frac{\zeta}{a}+(3-4\nu)\frac{z}{a}]R_2(z+\zeta)+\frac{2z\zeta}{a^2}R_3(z+\zeta) \end{aligned}\right\} \tag{2.11}$$

for all (z,ζ) in the region S given by (1.26)[1]. The required partial derivatives of $f(z,\zeta)$ and $g(z,\zeta)$ with respect to ζ are readily computed from (2.11) with the aid of the recursion relation

$$\dot{R}_n(t) = -\frac{1}{a}R_{n+1}(t) \quad (0<t<\infty), \tag{2.12}$$

---

1) As was pointed out in Section 1, the functions f and g may be continuously extended onto $\bar{S}$. This claim may be confirmed in the special case at hand by means of (2.11) and asymptotic estimates of $R_n(t)$ as $t\to 0$, which will be cited later on (See (2.18)).

which is implied by (2. 10). This computation furnishes

$$\left.\begin{aligned}
\frac{\partial}{\partial\zeta}f(z,\zeta)&=\frac{1}{(1-\nu)a^3}\{(1-2\nu)a^2[R_2(|z-\zeta|)-R_2(z+\zeta)]+a|z-\zeta|R_3(|z-\zeta|)\\
&\quad -a[\zeta+(1-4\nu)z]R_3(z+\zeta)-2z\zeta R_4(z+\zeta)\}\quad (0\le z\le\ell,\ 0\le\zeta\le\ell,\ z\neq\zeta),\\
\frac{\partial}{\partial\zeta}g(z,\zeta)&=\frac{1}{a^3}\{(1-4\nu)a^2R_2(|z-\zeta|)-(1-4\nu+8\nu^2)a^2R_2(z+\zeta)+a|z-\zeta|R_3(|z-\zeta|)\\
&\quad -(1-4\nu)a(z+\zeta)R_3(z+\zeta)-2z\zeta R_4(z+\zeta)\}\quad (0\le z\le\ell,\ 0\le\zeta\le\ell,\ z\neq\zeta).
\end{aligned}\right\}\ (2.13)$$

We adjoin here the analogous representation for the partial derivative of $f(z,\zeta)$ with respect to z, which will also be needed subsequently.

$$\left.\begin{aligned}
\frac{\partial}{\partial z}f(z,\zeta)&=\frac{-1}{(1-\nu)a^3}\{(1-2\nu)a^2[R_2(|z-\zeta|)-R_2(z+\zeta)]+a|z-\zeta|R_3(|z-\zeta|)\\
&\quad -a[\zeta-(3-4\nu)z]R_3(z+\zeta)+2z\zeta R_4(z+\zeta)\}\quad (0\le z\le\ell,\ 0\le\zeta\le\ell,\ z\neq\zeta).
\end{aligned}\right\}\ (2.14)$$

It is essential for numerical purposes, as well as for the asymptotic study of the actual bar-force p near the ends of the embedded bar-segment, to examine in detail the singular behavior at $z=\zeta$ of the partial derivatives listed in (2. 13), (2. 14). This behavior, in turn, is evidently governed by the asymptotic character of $R_n(t)$ as $t\to 0$. The functions R_n, introduced through (2. 10), are expressible in terms of the complete elliptic integrals of the first and second kind. Indeed, with

$$\left.\begin{aligned}
K(k)&=\int_0^{\pi/2}\frac{d\varphi}{\sqrt{1-k^2\sin^2\varphi}},\quad E(k)=\int_0^{\pi/2}\sqrt{1-k^2\sin^2\varphi}\,d\varphi,\\
k\equiv k(t)&=\frac{2a}{\sqrt{t^2+4a^2}}\quad (0<t<\infty),
\end{aligned}\right\}\ (2.15)^{1}$$

---

1) Our previous use of "E" for the entire space ought not to cause confusion.

one has[1]

$$\left.\begin{aligned} R_1(t)&=\frac{1}{2}-\frac{t}{\pi ak}[K(k)-E(k)] \quad (0<t<\infty),\\ R_2(t)&=\frac{1}{\pi k}[(2-k^2)K(k)-2E(k)] \quad (0<t<\infty),\\ R_3(t)&=-\frac{tk}{2\pi a}K(k)+\frac{a(2-k^2)}{\pi tk}E(k) \quad (0<t<\infty),\\ R_4(t)&=\frac{k^3}{4\pi}K(k)+\frac{k}{2\pi}[2(a/t)^2-k^2]E(k) \quad (0<t<\infty). \end{aligned}\right\} \quad (2.16)$$

Equations (2.16) confirm the analytic character of R_n (n=1, 2, 3, 4) on $(0, \infty)$. Now, from the last of (2.15) and familiar asymptotic estimates[2] of K(k), E(k) as $k\to 1$, follows

$$\left.\begin{aligned} K(k(t))&=-\log(t/8a)+O(t^2\log t) \text{ as } t\to 0,\\ E(k(t))&=1+O(t^2\log t) \text{ as } t\to 0. \end{aligned}\right\} \quad (2.17)$$

Combining (2.16) and (2.17), one thus arrives at the estimates

$$\left.\begin{aligned} R_1(t)&=\frac{1}{2}+O(t\log t) \text{ as } t\to 0,\\ R_2(t)&=-\frac{1}{\pi}[\log(t/8a)+2]+O(t^2\log t) \text{ as } t\to 0,\\ R_3(t)&=\frac{a}{\pi t}+O(t\log t) \text{ as } t\to 0,\\ R_4(t)&=\frac{a^2}{\pi t^2}+O(\log t) \text{ as } t\to 0 \end{aligned}\right\} \quad (2.18)$$

Equations (2.18) enable one to remove from the partial derivatives (2.13), (2.14), in closed elementary form, those contributions that become unbounded as $\zeta\to z$ $(0\le z\le \ell)$. We now cite the decompositions thus established.

---

1) See Eason, Noble, and Sneddon [11] for the first three of (2.16); the last of (2.16) is easily deduced from the preceding one with the aid of (2.12), (2.15).

2) See, for example, Oberhettinger and Magnus [12], p. 3.

$$\left.\begin{aligned}
&\frac{\partial}{\partial\zeta}f(z,\zeta)=-\frac{1}{\pi(1-\nu)a}\{(1-2\nu)\log[|z-\zeta|/(z+\zeta)]+\pi F(z,\zeta)\},\\
&\frac{\partial}{\partial\zeta}g(z,\zeta)=-\frac{1}{\pi a}\{(1-4\nu)\log[|z-\zeta|/8a]-(1-4\nu+8\nu^2)\log[(z+\zeta)/8a]\\
&\qquad\qquad +\pi G(z,\zeta)\}\quad(0\le z\le l,\ 0\le\zeta\le l,\ z\ne\zeta),
\end{aligned}\right\}\tag{2.19}$$

$$\left.\begin{aligned}
&\frac{\partial}{\partial z}f(z,\zeta)=\frac{1}{\pi(1-\nu)a}\{(1-2\nu)\log[|z-\zeta|/(z+\zeta)]+\pi H(z,\zeta)\}\\
&\qquad\qquad (0\le z\le l,\ 0\le\zeta\le l,\ z\ne\zeta),
\end{aligned}\right\}\tag{2.20}$$

where F, G, H, are new functions to be discussed presently. Let S' be the plane region obtained by deleting the origin from the closed square[1] $\bar{S}$, so that

$$S'=\{(z,\zeta)\,|\,0<z\le l,\ 0<\zeta\le l\}.\tag{2.21}$$

The functions F, G, and H are bounded and continuous on S'; moreover, for any fixed direction of approach, they possess limits as $(z,\zeta)\to(0,0)$. Explicit representations are needed merely for F and G:

$$\left.\begin{aligned}
&F(z,\zeta)=-(1-2\nu)\{R_2(|z-\zeta|)-R_2(z+\zeta)+\frac{1}{\pi}\log[|z-\zeta|/(z+\zeta)]\}\\
&\quad-\frac{1}{a^2}\{a|z-\zeta|R_3(|z-\zeta|)-a[\zeta+(1-4\nu)z]R_3(z+\zeta)-2z\zeta R_4(z+\zeta)\}\\
&\qquad\qquad (0\le z\le l,\ 0\le\zeta\le l,\ z\ne\zeta),\\
&F(z,z)=\frac{1-4\nu}{\pi}+(1-2\nu)[R_2(2z)+\frac{1}{\pi}\log(z/4a)]\\
&\quad+\frac{2}{a^2}[(1-2\nu)azR_3(2z)+z^2R_4(2z)]\ (0<z\le l),\ F(0,0+)=0;
\end{aligned}\right\}\tag{2.22}$$

$$\left.\begin{aligned}
&G(z,\zeta)=-(1-4\nu)\{R_2(|z-\zeta|)+\frac{1}{\pi}\log[|z-\zeta|/8a]\}\\
&\quad+(1-4\nu+8\nu^2)\{R_2(z+\zeta)+\frac{1}{\pi}\log[(z+\zeta)/8a]\}-\frac{1}{a^2}\{a|z-\zeta|R_3(|z-\zeta|)
\end{aligned}\right\}\tag{2.23}$$

---

[1] Recall (1.26).

$$-(1-4\nu)a(z+\zeta)R_3(z+\zeta)-2z\zeta R_4(z+\zeta)\}\ (0\le z\le\ell,\ 0\le\zeta\le\ell,\ z\neq\zeta),$$

$$G(z,z)=\frac{1-8\nu}{\pi}+(1-4\nu+8\nu^2)[R_2(2z)+\frac{1}{\pi}\log(z/4a)]$$

$$+\frac{2}{a^2}[(1-4\nu)azR_3(2z)+z^2R_4(2z)]\ (0<z\le\ell),\ G(0,0+)=-\frac{4\nu(1+4\nu)}{\pi}.\qquad (2.23)\ \text{cont.}$$

Equations (2.19), (2.22), (2.23), together with the elliptic-integral representation of R_n (n=2, 3, 4) contained in (2.16), supply – in a form suited to numerical purposes – the kernels $\partial f(z,\zeta)/\partial\zeta$ and $\partial g(z,\zeta)/\partial\zeta$ involved in (1.27), (1.28) for the case of a bar of circular cross-section. Further, the values $f(z,0)$, $g(z,0)$ $(0\le z\le\ell)$, which are also needed in connection with (1.27), (1.28), are computable from (2.11), (2.16) for $0<z\le\ell$, while

$$f(0+,0)=1,\ \ g(0+,0)=(1-2\nu)^2, \qquad (2.24)^{1}$$

as is easily verified on the basis of (2.11), (2.18). The Fredholm integral equation (1.27), which determines the fictitious bar-force $p_*(z)$ $(0\le z\le\ell)$, may now be solved numerically for any admissible choice[2] of the elastic constants η', η, and ν. To accomplish this task the range of integration $[0,\ell]$ in (1.27) was partitioned uniformly. The contribution to the improper integral arising from the (integrable) logarithmic singularity[3] of the kernel $\partial g(z,\zeta)/\partial\zeta$ at $z=\zeta$ was then evaluated in closed elementary form (in terms of the values of p_* at the mesh-points of the partition) upon replacing p_* by a continuous, piecewise linear function. On the other hand, the ordinary trapezoidal rule was used to compute

---

1) Note the agreement between the first of (2.24) and the last of (1.30).

2) Recall from (1.4) that $\eta_*=\eta'-\eta\ge 0$ and see the footnote attached to (1.14).

3) See (2.19).

the contribution to the integral under consideration stemming from the bounded portion G of the kernel, which is given by (2.23). In this manner (1.27) was reduced to a system of linear algebraic equations, whose solution was obtained on an electronic computer. Once $p_*(z)$ $(0\le z\le \ell)$ had been so determined, the desired actual bar-force p(z) $(0\le z\le \ell)$ was found from (1.28) by means of a numerical evaluation of the improper integral in (1.28) that is strictly analogous to the numerical integration scheme described above.

Before proceeding to the results thus established, we investigate the asymptotic behavior of $\dot{p}(z)$ at the endpoints $z=0$ and $z=\ell$ of the embedded bar-segment. Substituting for σ from (1.24) into (1.13) and differentiating the resulting identity with respect to z, one draws

$$\left.\begin{aligned}\dot{p}(z)=\frac{1}{\Sigma}\Big\{[p_o-p_*(0)]\frac{\partial f}{\partial z}\Big|_{(z,\,0)}+p_*(\ell)\frac{\partial f}{\partial z}\Big|_{(z,\,\ell)}\\ -\int_0^{\ell}\dot{p}_*(\zeta)\frac{\partial}{\partial z}f(z,\zeta)d\zeta\Big\}\quad (0<z<\ell).\end{aligned}\right\}\quad (2.25)$$

Moreover, for the bar of circular cross-section, $\partial f(z,\zeta)/\partial z$ admits the representation (2.20). Next, we suppose that for some fixed $\alpha>1$, $\dot{p}_*^{\alpha}$ is absolutely integrable on $[0,\ell]$ and invoke the Hölder inequality[1] to justify the estimate

$$\left.\begin{aligned}\Big|\int_0^{\ell}\dot{p}_*(\zeta)\frac{\partial}{\partial z}f(z,\zeta)d\zeta\Big|\le\Big[\int_0^{\ell}|\dot{p}_*(\zeta)|^{\alpha}d\zeta\Big]^{\frac{1}{\alpha}}\Big[\int_0^{\ell}\Big|\frac{\partial}{\partial z}f(z,\zeta)\Big|^{\beta}d\zeta\Big]^{\frac{1}{\beta}},\\ \alpha>1,\ \frac{1}{\alpha}+\frac{1}{\beta}=1,\ (0\le z\le\ell).\end{aligned}\right\}\quad (2.26)^2$$

---

1) See, for example, Beckenbach and Bellman [13], p. 21.

2) Note that the second integral in the right-hand member of (2.26) exists by virtue of (2.20), for every $\beta>0$. Further, it is not difficult to show that this integral is bounded for $0\le z\le\ell$.

Consequently, the integral in the right-hand member of (2.25) is bounded on $(0, \ell)$ under the foregoing rather weak assumption concerning $\dot{p}_*$. In these circumstances it follows from (2.25) and (2.20) that

$$\left.\begin{aligned} \dot{p}(z) &= O(1) \text{ as } z \to 0, \\ \dot{p}(z) &= \frac{(1-2\nu)p_*(\ell)}{2\pi(1-\nu)a}\log[(\ell-z)/a]+O(1) \text{ as } z \to \ell \end{aligned}\right\} \quad (2.27)$$

Next, it is essential to examine the manner in which the various physical parameters enter the solution of the problem under consideration. To focus attention on this issue, we now write

$$p(z)=p(z;p_o, a, \ell, \eta', \eta, \nu) \quad (0\le z\le \ell), \quad (2.28)$$

where, it will be recalled, the parametric arguments p_o, a, ℓ, η', η and ν, in this order, stand for the applied scalar bar-load, the radius of the bar, the length of the embedded bar-segment, Young's modulus of the bar, Young's modulus of the surrounding medium, and Poisson's ratio of the latter. It is clear from the structure of (1.27), (1.28), in view of (1.4), (2.11), (2.13), and (2.10), that the solution may be cast into the dimensionless form

$$p(z)/p_o=\psi(z/a;\, \ell/a, \eta'/\eta, \nu) \quad (0\le z/a\le \ell/a), \quad (2.29)$$

so that the dimensionless (normalized) bar-force $p(z)/p_o$ depends exclusively upon the dimensionless depth-coordinate z/a, the length-ratio ℓ/a, the stiffness-ratio η'/η, and the Poisson-ratio ν. The function ψ in (2.29) is independent of ℓ/a and ν for $\eta'/\eta=1$, i.e., if the bar and the embedding medium have the same modulus of elasticity. For this degenerate limiting case, (1.32), the first of (2.11), and (1.25) furnish

$$p(z)=2p_o\left[R_1(z)+\frac{z}{a}R_2(z)\right] \quad (0<z\le \ell), \quad p(0)=p_o, \quad (2.30)$$

with R_1, R_2 given by (2.15), (2.16).

We turn now to the discussion of illustrative numerical results for the decay of the actual bar-force p, which are depicted graphically in Figure 3 to Figure 8. The load-diffusion curves displayed in these diagrams show the normalized bar-force $p(z)/p_o$ as a function of the dimensionless depth-coordinate z/a for $0 \le z/a \le \ell/a$ and various choices of the dimensionless physical parameters ℓ/a, η'/η, ν. Each of the six figures under discussion refers to a single Poisson's ratio ν of the embedding medium, to two values of the length-ratio ℓ/a, and to four distinct choices of the stiffness-ratio η'/η. The thirty-six combinations of parameter-values covered by the graphs presented here are listed in the following table.

Figure 3: $\nu=0$; $\ell/a=5, 10$; $\eta'/\eta=1, 2, 4, 8$.

Figure 4: $\nu=0$; $\ell/a=10, 20$; $\eta'/\eta=1, 2, 4, 8$.

Figure 5: $\nu=\frac{1}{4}$; $\ell/a=5, 10$; $\eta'/\eta=1, 2, 4, 8$.

Figure 6: $\nu=\frac{1}{4}$; $\ell/a=10, 20$; $\eta'/\eta=1, 2, 4, 8$.

Figure 7: $\nu=\frac{1}{2}$; $\ell/a=5, 10$; $\eta'/\eta=1, 2, 4, 8$.

Figure 8: $\nu=\frac{1}{2}$; $\ell/a=10, 20$; $\eta'/\eta=1, 2, 4, 8$.

As is apparent from this table, the load-diffusion curves appropriate to $\ell/a=10$ in Figures 3, 5, 7 are, for comparison purposes, repeated in Figures 4, 6, 8.

All of the curves under consideration represent functions $p(z)/p_o$ that are steadily decreasing throughout their interval of definition $0 \le z/a \le \ell/a$. Further, in each instance,

$$p(0)/p_o=1, \quad p(\ell)/p_o>0, \qquad (2.31)^1$$

the first of (2.31), according to (1.31), being valid for a bar of arbitrary cross-section. Therefore, no part of the applied load is communicated to the embedding medium through bond-forces concentrated at z=0, whereas a portion of the load is transmitted to the surrounding solid through bond-forces concentrated at the terminal cross-section of the bar. The graphs indicate that this load-portion increases with the stiffness-ratio and is a decreasing function of the length-ratio; in the examples to which Figures 4, 6, 8 refer, the fraction of the load transferred at the embedded end of the bar is less than 10% for $\ell/a=10$ and less than 5% for $\ell/a=20$.

The absence of any concentrated load-transfer at z=0, predicted by the current solution, is interesting in view of the corresponding result encountered earlier in an analogous treatment of Reissner's plane load-transfer problem[2]: there, a substantial part of the load was found to be transmitted to the sheet at the junction of sheet and stringer. On the other hand, as was shown in [5], singular load-transfer at either end of the attached stringer-segment is precluded within Reissner's [2] original formulation of the plane problem.

For all illustrative examples considered here, the initial slope (at z=0) of the load-diffusion curve is finite in agreement with the first of (2.27); the infinity of the end-slope at $z=\ell$, predicted by the second

---

1) The analytical determination of $p(\ell)$, on the basis of (1.27), (1.28), appears to offer serious difficulties even for the circular bar. In the degenerate case $\eta'/\eta=1$, $p(\ell)$ for the circular bar is immediate from (2.30), (2.15), (2.16).

2) See Section 3 of [5].

of (2.27)[1] if $\nu \neq 1/2$, is not discernible on the scale of Figure 3 to Figure 6.

As is intuitively plausible, each of the diagrams reflects a less rapid diffusion of the load with rising values of the stiffness-ratio. Even for a relatively stiff bar of sufficiently large length-ratio, however, most of the load-transfer takes place in the vicinity of the surface of the embedding medium and – in this range – is quite insensitive to changes of the length-ratio. To illustrate this observation, we refer to Figure 6 ($\nu=1/4$) and regard the bar-radius as fixed. An inspection of the curves in this figure reveals that for $\eta'/\eta \leq 8$ and $\ell=20a$ over half of the applied load is transferred to the matrix by the bar-segment in the range $0 \leq z \leq 4a$. Further, the dashed curves appropriate to $\ell=10a$ are, in this range, practically indistinguishable from the corresponding solid curves[2], which pertain to $\ell=20a$. Accordingly, here very little benefit is derived from a doubling of the embedded bar-length. This finding, which is also borne out by the results given in Figure 4 and Figure 8, would appear to be significant for design purposes.

In conclusion we emphasize once more that the analysis carried out in this section is bound to be inadequate unless the length of the embedded segment of the bar is sufficiently large compared to the bar-diameter.

---

1) $p_*(\ell)$ was found not to vanish in the examples dealt with numerically.

2) The dashed and the solid curve for $\eta'/\eta=1$ are identical in all figures since here p is independent of the length-ratio, as well as of ν. See (2.30) and the remarks preceding (2.30).

Appendix: Proof of the limit-relations (1.23).

We indicate here a proof of the limit-relations (1.23) pertaining to the functions W_n (n=1,2,3) defined by (1.19), (1.20). In order not to detract from the essence of the proof, we shall confine our attention to a cross-sectional domain Π, the boundary $\partial\Pi$ of which is a simple closed curve with continuously varying curvature[1]. Accordingly, denoting by s the arc-length of $\partial\Pi$ (measured counter-clockwise from an arbitrarily chosen fixed point of the closed curve at hand) we assume that $\partial\Pi$ admits the parameterization

$$\partial\Pi: x_1=\lambda_1(s),\ x_2=\lambda_2(s)\ (0\le s\le s_o), \tag{1}$$

where λ_1 and λ_2 are functions twice continuously differentiable on $[0, s_o]$, while

$$\lambda_\beta(0)=\lambda_\beta(s_o),\ \dot\lambda_\beta(0)=\dot\lambda_\beta(s_o),\ \ddot\lambda_\beta(0)=\ddot\lambda_\beta(s_o)\ (\beta=1,2), \tag{2}$$

s_o being the total length of $\partial\Pi$. The curvature $\varkappa$ of $\partial\Pi$ is given by

$$\varkappa(s)=\dot\lambda_1(s)\ddot\lambda_2(s)-\dot\lambda_2(s)\ddot\lambda_1(s) \tag{3}$$

and, for convenience, we set

$$m=\max_{0\le s\le s_o}|\varkappa(s)|,\ t_o=\frac{1}{2m}. \tag{4}$$

Next, let Π' be the closed band-shaped sub-region of $\bar\Pi$ consisting of all points in $\bar\Pi$ whose perpendicular distance from $\partial\Pi$ fails to exceed t_o, i.e.,

$$\Pi'=\{(x_1,x_2)|(x_1,x_2)\in\bar\Pi,\ [x_1-\lambda_1(s)]^2+[x_2-\lambda_2(s)]^2\le t_o^2\ (0\le s\le s_o)\}. \tag{5}$$

Further, for every point (x_1, x_2) in Π', let $s(x_1, x_2)$ be the arc-length

---

1) The following argument is easily generalized to accommodate a boundary $\partial\Pi$ that exhibits corners, but is composed of a finite number of arcs with continuous curvature.

associated with that orthogonal projection of (x_1, x_2) onto $\partial\Pi$ which has the smallest distance from (x_1, x_2); also, let $t(x_1, x_2)$ be the distance of this orthogonal projection from the point (x_1, x_2). Evidently, $s(x_1, x_2)$ and $t(x_1, x_2)$ define an orthogonal curvilinear coordinate-net on Π'. The underlying coordinate transformation is characterized by

$$\left.\begin{aligned} x_1(s,t)&=\lambda_1(s)-t\dot{\lambda}_2(s),\\ x_2(s,t)&=\lambda_2(s)+t\dot{\lambda}_1(s)\quad (0\le s<s_o,\ 0\le t\le t_o),\end{aligned}\right\} \tag{6}$$

and the mapping (6) is one-to-one on Π'; indeed, its Jacobian obeys

$$J(s,t)=\frac{\partial x_1}{\partial s}\frac{\partial x_2}{\partial t}-\frac{\partial x_1}{\partial t}\frac{\partial x_2}{\partial s}=1-t\varkappa(s)>0\quad (0\le s<s_o,\ 0\le t\le t_o), \tag{7}$$

the inequality being a consequence of (4). Finally, for every (x_1, x_2) in Π, we adopt the notation

$$\left.\begin{aligned} \Sigma(x_1,x_2)&=\{(\xi_1,\xi_2)\,|\,(\xi_1-x_1)^2+(\xi_2-x_2)^2\le\mu^2(x_1,x_2)\},\\ \mu(x_1,x_2)&=\min\sqrt{(\xi_1-x_1)^2+(\xi_2-x_2)^2},\quad (\xi_1,\xi_2)\in\partial\Pi,\end{aligned}\right\} \tag{8}$$

so that $\Sigma(x_1, x_2)$ stands for the interior of the largest closed circular disk contained in $\bar{\Pi}$ and centered at (x_1, x_2).

Having disposed of these geometric preliminaries, we recall from (1.20), (1.19), and (1.3) that

$$W_1(z)=\frac{1}{A}\int_{\Pi}V_1(x_1,x_2,z)\,dA\quad (0<|z|<\infty), \tag{9}$$[1]

where

---

[1] Note that we now write (x_1, x_2, x_3) in place of the single vectorial argument $\underset{\sim}{x}$.

$$V_1(x_1, x_2, z)=\frac{z}{A}\int_{\Pi}(\rho^2+z^2)^{-3/2}dA_{\underset{\sim}{\xi}},\quad \rho^2\equiv(x_1-\xi_1)^2+(x_2-\xi_2)^2 \qquad (10)^1$$

for all $(x_1, x_2)\in\Pi$ and all $z\neq 0$. From (9) follows the estimate

$$|W_1(z)-\frac{2\pi}{A}h(z)|\leq M(z)+N(z)\ \ (0<|z|<\infty), \qquad (11)$$

in which

$$\left.\begin{aligned} M(z)&=\frac{1}{A}\int_{\Pi-\Pi'}|V_1(x_1, x_2, z)-\frac{2\pi}{A}h(z)|dA,\\ N(z)&=\frac{1}{A}\int_{\Pi'}|V_1(x_1, x_2, z)-\frac{2\pi}{A}h(z)|dA\ \ (0<|z|<\infty),\end{aligned}\right\} \qquad (12)$$

whereas h is the step-function defined in (1.25). In order to establish the first two of (1.23) it suffices to show that M(z) and N(z) tend to zero as $z\to 0$.

Now fix (x_1, x_2) in Π, write Σ and μ in place[2] of $\Sigma(x_1, x_2)$ and $\mu(x_1, x_2)$, and infer from (10) that

$$V_1(x_1, x_2, z)=\frac{2\pi z}{A}\int_0^{\mu}\frac{\rho d\rho}{(\rho^2+z^2)^{3/2}}+\frac{z}{A}\int_{\Pi-\Sigma}(\rho^2+z^2)^{-3/2}dA_{\underset{\sim}{\xi}} \qquad (13)$$

for every $z\neq 0$. However,

$$\left.\begin{aligned} z\int_0^{\mu}\frac{\rho d\rho}{(\rho^2+z^2)^{3/2}}&=h(z)-\frac{z}{\sqrt{\mu^2+z^2}}\ \ (z\neq 0),\\ \int_{\Pi-\Sigma}(\rho^2+z^2)^{-3/2}dA_{\underset{\sim}{\xi}}&<2\pi\int_{\mu}^{\infty}\frac{\rho d\rho}{(\rho^2+z^2)^{3/2}}=\frac{2\pi}{\sqrt{\mu^2+z^2}}\ \ (z\neq 0).\end{aligned}\right\} \qquad (14)$$

Combining (13) and (14), one has

---

1) The subscript $\underset{\sim}{\xi}$ attached to the element of area is to indicate that (ξ_1, ξ_2) are the variables of integration.

2) See (8) for the definition of $\Sigma(x_1, x_2)$ and $\mu(x_1, x_2)$.

$$|V_1(x_1, x_2, z) - \frac{2\pi}{A} h(z)| < \frac{4\pi|z|}{A\sqrt{\mu^2+z^2}} \quad (0<|z|<\infty). \tag{15}$$

But, according to (5) and (8),

$$0<t_o<\mu(x_1, x_2) \text{ for all } (x_1, x_2)\in\Pi-\Pi'. \tag{16}$$

Consequently, if A' stands for the area of Π', (15) and the first of (12) furnish

$$M(z)<\frac{4\pi(A-A')|z|}{A^2\sqrt{t_o^2+z^2}}=o(1) \text{ as } z\to 0. \tag{17}$$

On the other hand, the second of (12), together with (15) and the second of (8), yield the estimate

$$N(z)<\frac{4\pi|z|}{A^2} I(z), \quad I(z)=\int_{\Pi'} \frac{dA}{\sqrt{t^2(x_1, x_2)+z^2}} \quad (0<|z|<\infty) \tag{18}$$

since[1] $\mu(x_1, x_2)=t(x_1, x_2)$ for all (x_1, x_2) in Π'. Changing the variables of integration in (18) from (x_1, x_2) to the curvilinear coordinates (s, t) introduced in (6) and bearing (7) in mind, we arrive at

$$I(z)=\int_0^{t_o}\int_0^{s_o} \frac{1-t\varkappa(s)}{\sqrt{t^2+z^2}}\, ds\, dt \quad (0<|z|<\infty). \tag{19}$$

From (19) and (4), in turn, follows the estimate

$$0<I(z)\le\frac{3s_o}{2}\int_0^{t_o}\frac{dt}{\sqrt{t^2+z^2}}=\frac{3s_o}{2}\left[\log(t_o+\sqrt{t_o^2+z^2})-\log|z|\right] \quad (0<|z|<\infty). \tag{20}$$

Combining (18) and (20), we reach

$$N(z)<\frac{4\pi|z|}{A^2} I(z)=o(1) \text{ as } z\to 0. \tag{21}$$

---

1) Recall the geometric significance of the curvilinear coordinate $t(x_1, x_2)$ associated with the mapping (6).

Finally, (11), (17), and (21) assure that

$$\lim_{z\to 0}\left[W_1(z)-\frac{2\pi}{A}h(z)\right]=0, \tag{22}$$

which confirms the first two of (1.23). The remaining limit-relation in (1.23) may be established by similar means.

References

[1] E. Melan, Ein Beitrag zur Theorie geschweisster Verbindungen, Ingenieur Archiv, 3 (1932), 2, p. 123.

[2] E. Reissner, Note on the problem of the distribution of stress in a thin stiffened elastic sheet, Proceedings, National Academy of Sciences, 26 (1940), p. 300.

[3] R. Muki and E. Sternberg, Transfer of load from an edge-stiffener to a sheet – a reconsideration of Melan's problem, Journal of Applied Mechanics, 34 (1967), 3, p. 679.

[4] R. Muki and E. Sternberg, On the stress analysis of overlapping bonded elastic sheets, International Journal of Solids and Structures, 4 (1968), 1, p. 75.

[5] R. Muki and E. Sternberg, On the diffusion of load from a transverse tension-bar into a semi-infinite elastic sheet, Journal of Applied Mechanics, 35 (1968), 4, p. 737.

[6] R. Muki and E. Sternberg, On the diffusion of an axial load from an infinite cylindrical bar embedded in an elastic medium, Technical Report No. 16, Contract Nonr-220(58), California Institute of Technology, September 1968. To appear in International Journal of Solids and Structures.

[7] R. D. Mindlin, Force at a point in the interior of a semi-infinite solid, Physics, 7 (1936), p. 195.

[8] R. D. Mindlin, Force at point in the interior of a semi-infinite solid, Proceedings, First Midwestern Conference of Solid Mechanics, Urbana, Illinois, 1953, p. 56.

[9] G. N. Watson, A treatise on the theory of Bessel functions, Second edition, Cambridge University Press, Cambridge, 1962.

[10] H. Weber, Über die Besselschen Funktionen und ihre Anwendungen auf die Theorie der elektrischen Ströme, Journal für die reine und angewandte Mathematik, LXXV (1873), p. 75.

[11] G. Eason, B. Noble and I. N. Sneddon, On certain integrals of Lipschitz-Hankel type involving products of Bessel functions, Philosophical Transactions of the Royal Society of London, Series A, 247 (1955), 935, p. 529.

[12] F. Oberhettinger and W. Magnus, Anwendung der Elliptischen Funktionen in Physik und Technik, Springer-Verlag, Berlin, 1949.

[13] E. F. Beckenbach and R. Bellman, Inequalities, Springer-Verlag, Berlin, 1965.

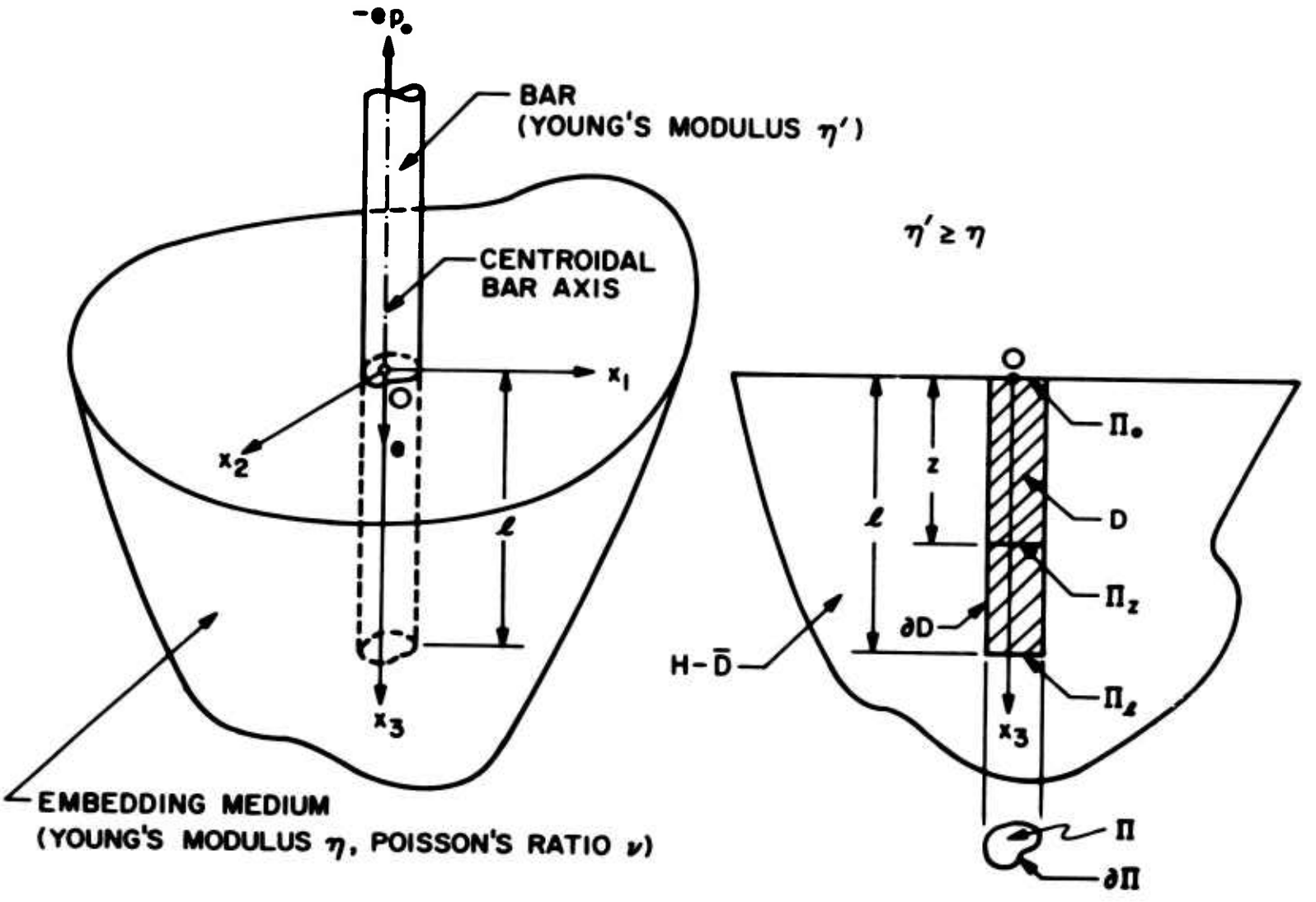

FIGURE 1. GEOMETRY OF BAR AND EMBEDDING MEDIUM

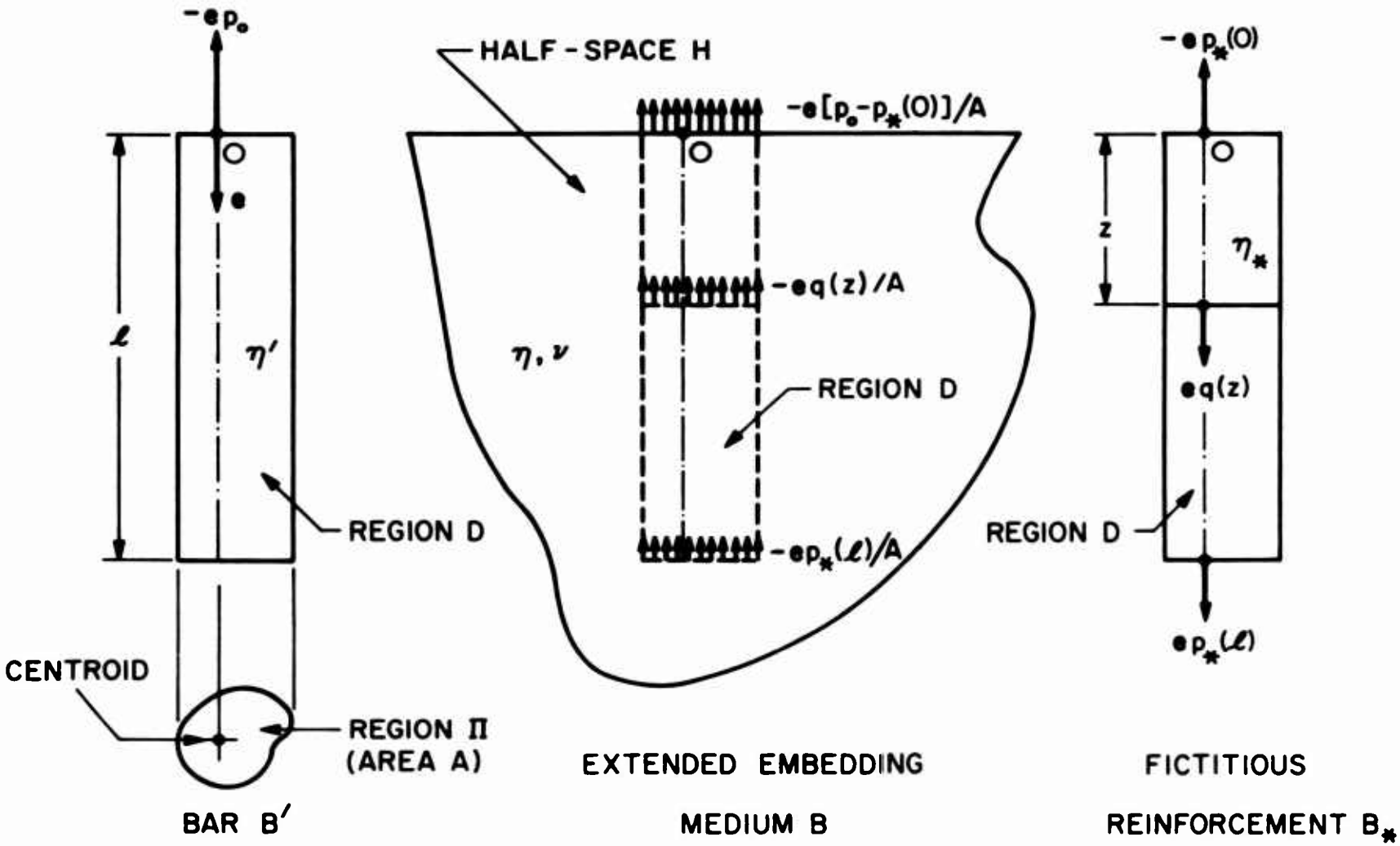

FIGURE 2. BAR, EXTENDED EMBEDDING MEDIUM, FICTITIOUS REINFORCEMENT

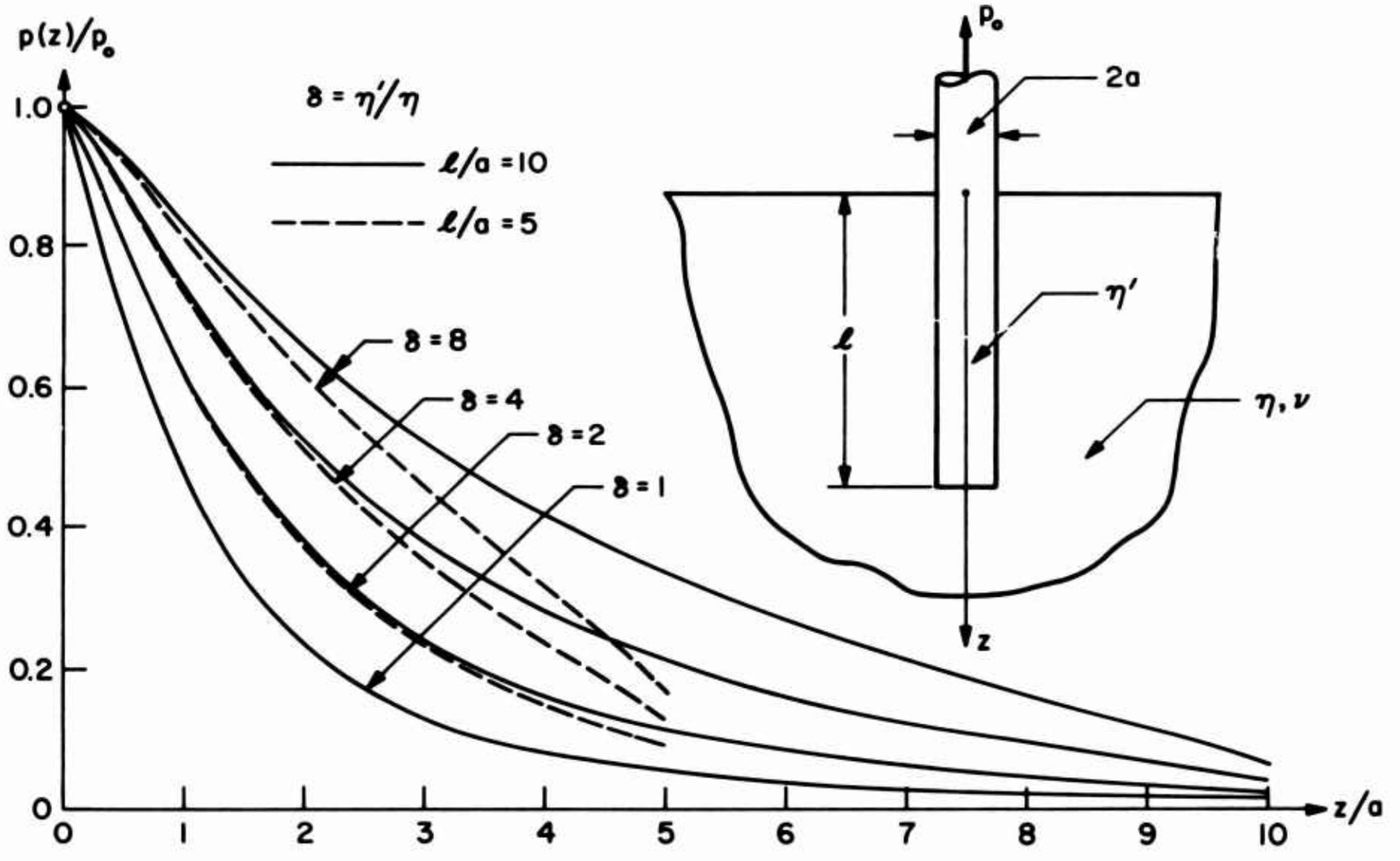

FIGURE 3. CIRCULAR BAR: $\nu = 0$, $\ell/a = 5$, $\ell/a = 10$

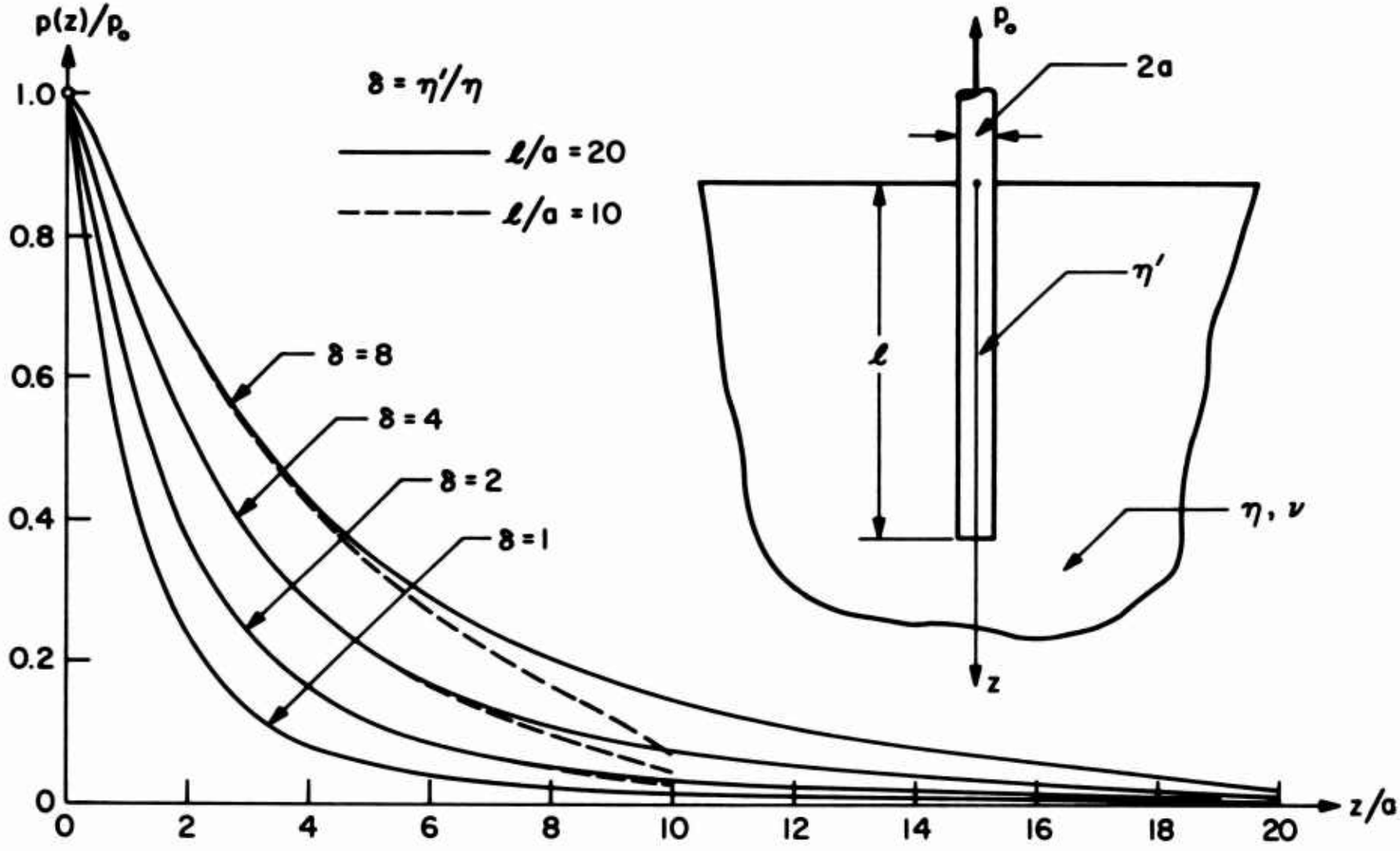

FIGURE 4. CIRCULAR BAR: $\nu = 0$, $\ell/a = 10$, $\ell/a = 20$

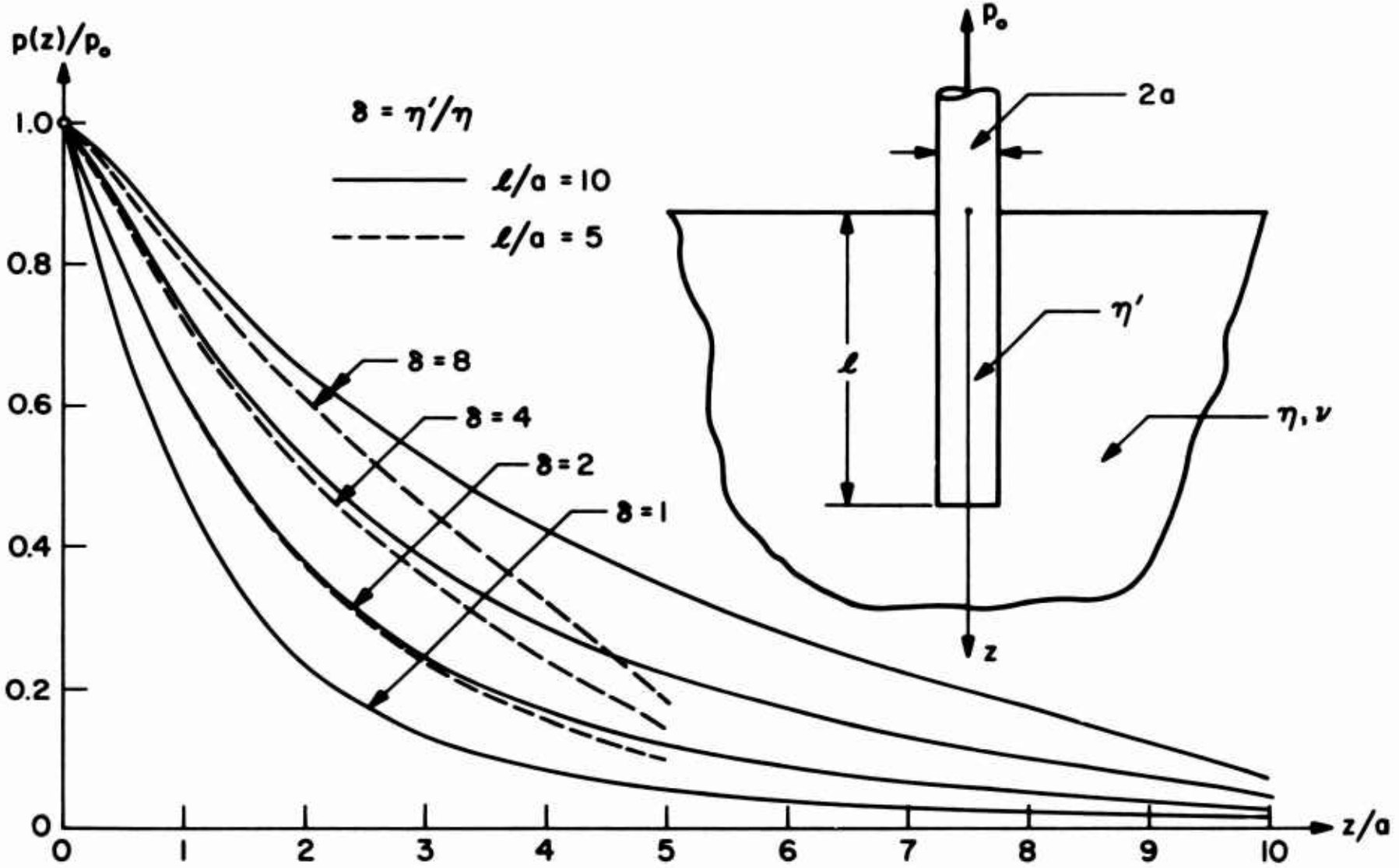

FIGURE 5. CIRCULAR BAR: $\nu = 1/4$, $\ell/a = 5$, $\ell/a = 10$

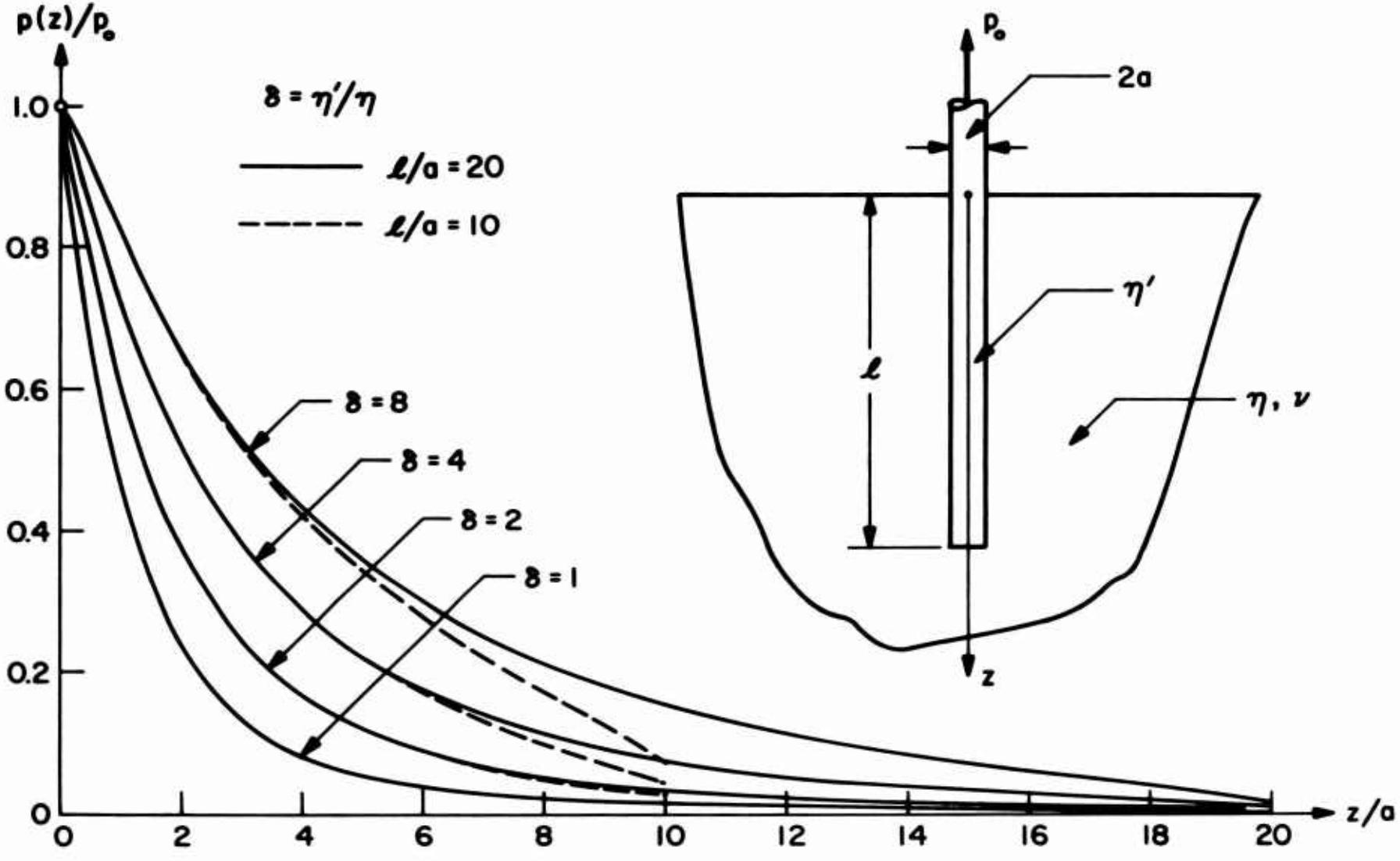

FIGURE 6. CIRCULAR BAR: $\nu = 1/4$, $\ell/a = 10$, $\ell/a = 20$

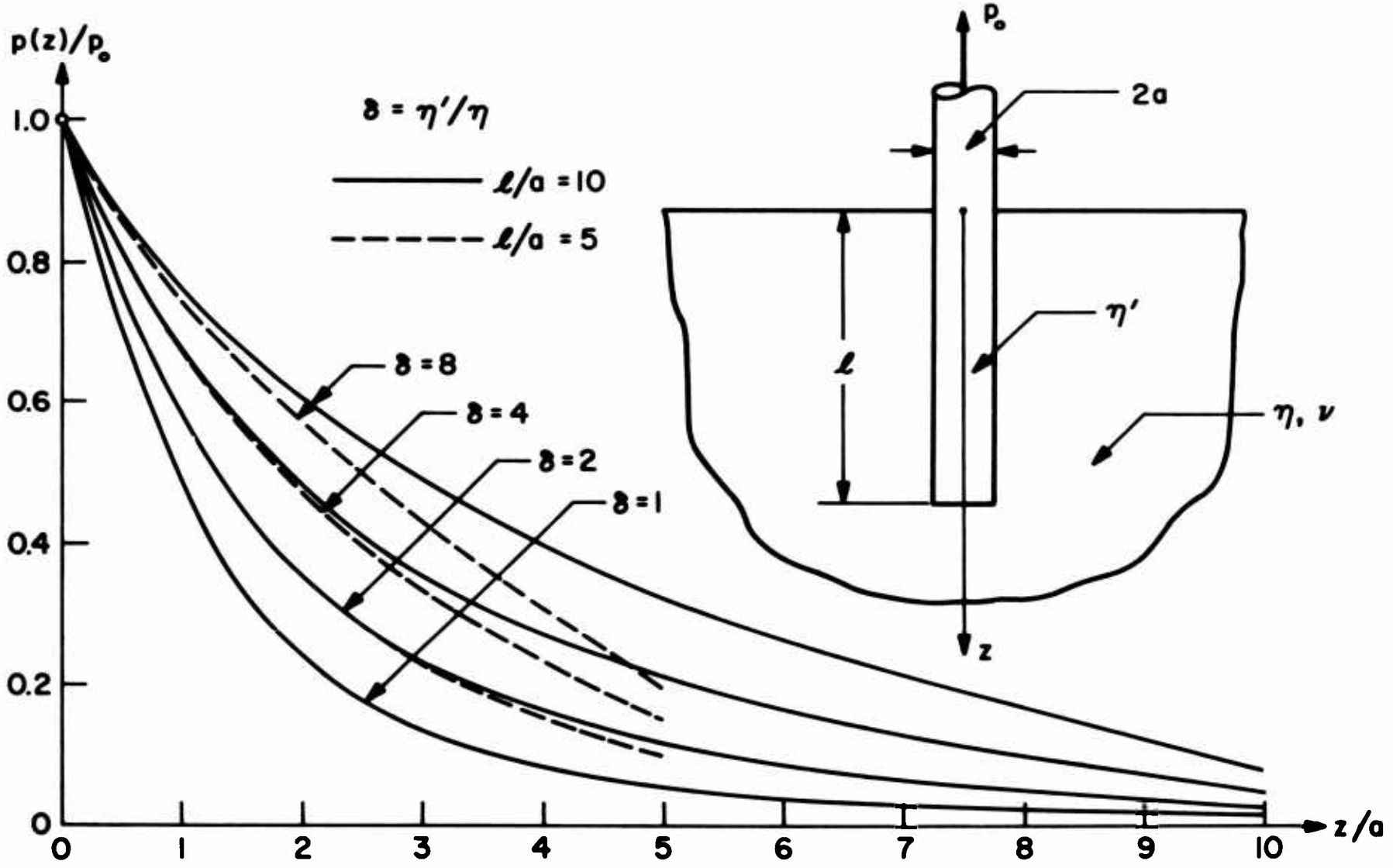

FIGURE 7. CIRCULAR BAR: $\nu = 1/2$, $\ell/a = 5$, $\ell/a = 10$

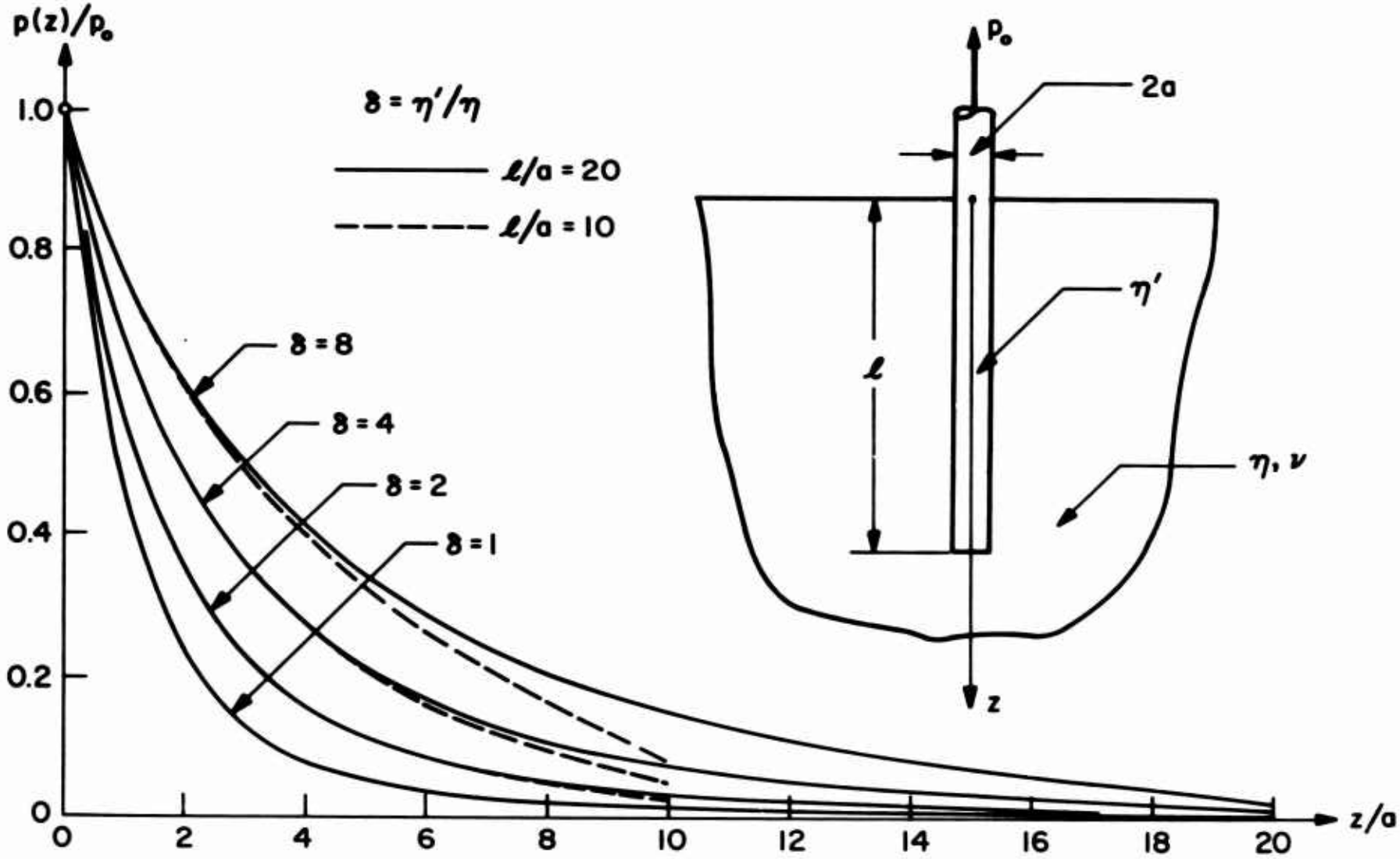

FIGURE 8. CIRCULAR BAR: $\nu = 1/2$, $\ell/a = 10$, $\ell/a = 20$

Unclassified
Security Classification

DOCUMENT CONTROL DATA - R & D

(Security classification of title, body of abstract and indexing annotation must be entered when the overall report is classified)

1 ORIGINATING ACTIVITY (Corporate author) California Institute of Technology	2a. REPORT SECURITY CLASSIFICATION Unclassified 2b. GROUP

3 REPORT TITLE

Elastostatic load-transfer to a half-space from a partially embedded axially loaded rod.

4 DESCRIPTIVE NOTES (Type of report and inclusive dates)
Research Report

5 AUTHOR(S) (First name, middle initial, last name)

Muki, Rokuro and Sternberg, Eli

6 REPORT DATE April 1969	7a. TOTAL NO. OF PAGES 41	7b. NO. OF REFS 13
8a. CONTRACT OR GRANT NO Nonr-220(58) b. PROJECT NO NR-064-431 c. d.	9a. ORIGINATOR'S REPORT NUMBER(S) No. 18 9b. OTHER REPORT NO(S) (Any other numbers that may be assigned this report)	

10 DISTRIBUTION STATEMENT

Distribution of this document is unlimited.

11 SUPPLEMENTARY NOTES	12 SPONSORING MILITARY ACTIVITY Office of Naval Research Washington, D. C. 20360

13 ABSTRACT

This investigation is concerned with the diffusion of an axial load from a bar of arbitrary uniform cross-section that is immersed in, up to a finite depth, and bonded to a semi-infinite solid of distinct elastic properties. The bar is perpendicular to the plane boundary of the embedding medium. The determination of the desired resultant force in the submerged bar-segment is reduced to a Fredholm integral equation by means of an approximative scheme developed and tested earlier in connection with a more elementary three-dimensional load-transfer problem. Extensive numerical results illustrating the decay of the bar-force, appropriate to various choices of the governing geometric and material parameters, are presented for the particular case of a bar of circular cross-section.

DD FORM 1 NOV 65 1473 (PAGE 1)

S/N 0101-807-6801

Unclassified
Security Classification

14. KEY WORDS	LINK A		LINK B		LINK C	
	ROLE	WT	ROLE	WT	ROLE	WT
Elastostatics, load-transfer, rod, half-space, three-dimensional						